Contents lists available at ScienceDirect

Food Research International

journal homepage: www.elsevier.com

# Physico-chemical and structural properties of crystalline inulin explain the stability of *Lactobacillus plantarum* during spray-drying and storage

Nelson Romano[a], Pablo Mobili[a], Maria Elvira Zuñiga-Hansen[b, c], Andrea Gómez-Zavaglia[a, *]

[a] Center for Research and Development in Food Cryotechnology (CIDCA, CCT-CONICET La Plata), RA1900 La Plata, Argentina
[b] School of Biochemical Engineering, Pontificia Universidad Católica de Valparaíso, Avenida Brasil 2147, Valparaíso, Chile
[c] Centro Regional de Estudios en Alimentos Saludables (CREAS), Conicyt-Regional, Gore Región de Valparaíso, R06i1004, Blanco 1623, Valparaíso, Chile

ARTICLE INFO

*Keywords:*
Crystalline
Amorphous
Inulin matrices
*Lactobacillus plantarum*
Spray-drying

ABSTRACT

The stabilizing capacity of crystalline inulin during spray-drying and storage of *Lactobacillus plantarum* CIDCA 83114 was assessed. In a first step, the physical properties of the matrices were investigated, using amorphous inulin as control. Melting and glass transition temperatures, water sorption isotherms, water activity, and infrared spectra were determined. Microorganisms were spray-dried at a pilot scale in both amorphous and crystalline matrices. After that, scanning electronic and confocal microsopies provided a full landscape about the interactions between microorganisms and crystals, and also the bacterial location within the amorphous matrices. The technological properties of the dehydrated microorganisms (culturability and acidification capacity) during storage at different water activities were also evaluated.

Both amorphous and crystalline inulins were adequate matrices to stabilize microorganisms. However, crystalline inulin was more stable than amorphous one, especially when the storage temperature was close to the glass transition temperature, resulting in a better matrix to protect microorganisms during pilot spray-drying and storage. Furthermore, no accumulation of insoluble inulin was observed after resuspending the dehydrated microorganisms in crystalline inulin matrices, which appears as a clear technological advantage with regard to the amorphous one.

Considering the prebiotic character of inulin and the probiotic properties of *L. plantarum* CIDCA 83114, this work developed an integrated approach, both from a fundamental and from an applied viewpoint, supporting the incorporation of such ingredients in the formulation of food products.

## 1. Introduction

Inulin is a natural polysaccharide present in consumed vegetables and fruits, such as onion, leek, garlic, banana, wheat, rye and barley, as well as in many roots, including Jerusalem artichoke, chicory root, garlic, asparagus root, satisfy and dandelion root [Kaur & Gupta, 2002]. From a chemical point of view, this polysaccharide belongs to the fructan family of carbohydrates and is composed of fructose units linked by (2→1)-β-glycosidic bonds, and a D-glycosyl moiety at the end [Romano, Santos, Mobili, Vega, & Gómez-Zavaglia, 2016]. The length of the fructose chains ranges from 2 to 60 monomers. As it is not digested in the upper part of the gastro-intestinal tract, inulin is considered dietary fiber [Meyer, Bayarri, Tárrega, & Costell, 2011]. Large chain inulins [those with degree of polymerization (DP) >10] are relatively hydrophobic, being able to form gels that increase the viscosity and enhance the organoleptic properties of foods. Because of such physico-chemical properties, inulins have also been used to improve the food texture in replacement of saturated fats [Franck, 2002]. Furthermore, the relatively high glass transition temperature ($T_g$) of amorphous inulin, in combination with its flexible backbone makes it a good stabilizer of pharmaceuticals and protein-based foods [Hinrichs, Prinsen, & Frijlink, 2001]. All these aspects underline the versatility of inulin as a food ingredient in the formulation of functional foods [Kelly, 2008, 2009; Kolida & Gibson, 2007; Roberfroid & Delzenne, 1998; Seifert & Watzl, 2007].

*Abbreviations:* DP, degree of polymerization; HPAEC, High Performance Anion Exchange Chromatography; $T_g$, glass transition temperature; MRS, de Man, Rogosa, Sharpe; $a_w$, water activity; GAB, Guggenheim-Anderson-de Boer; $T_m$, melting temperature; DSC, differential scanning calorimetry; d.m., dry matter; FTIR, Fourier transform infrared spectroscopy; ATR, Attenuated total reflection; SEM, scanning electronic microscopy; ANOVA, analysis of variance; A.U., absorbance units.

* Corresponding author at: Calle 47 y 116 La Plata, Buenos Aires 1900, Argentina.
*Email address:* angoza@qui.uc.pt (A. Gómez-Zavaglia)

https://doi.org/10.1016/j.foodres.2018.07.007
Received 12 May 2018; Received in revised form 2 July 2018; Accepted 4 July 2018
Available online xxx
0963-9969/ 

Lactic acid bacteria have an important role in the food and pharmaceutical industries, as they are widely used as starters for the manufacturing of food and probiotic products. For this reason, adequate preservation processes are necessary to stabilize these microorganisms and minimize viability and functionality losses during storage. Spray-drying is a dehydration technique increasingly used to dehydrate lactic acid bacteria [Meng, Stanton, Fitzgerald, Daly, & Ross, 2008; Morgan, Herman, White, & Vesey, 2006; Golowczyc et al., 2011; Golowczyc, Silva, Teixeira, De Antoni, & Abraham, 2011; Sosa et al., 2016; Quintana, Gerbino, & Gomez-Zavaglia, 2017]. This cost-effective process leads to the transformation of liquid systems (*i.e.*, solutions, dispersions, emulsions) into dry particulate flowable powders when they get in contact with a drying medium (air) at high temperatures. It is particularly useful for the production of starters at a large scale due to the low energy consumption and the reduced costs of storage and transportation [Santivarangkna, Higl, & Foerst, 2008]. The presence of carbohydrates in the dehydration media increases the stability of the spray-dried microorganisms, because of their capacity to create amorphous structures that inhibit or slow down deterioration processes [Crowe, Carpenter, & Crowe, 1998; Fazaeli, Emam-Djomeh, Ashtari, & Omid, 2012; Rajam & Anandharamakrishnan, 2015; Chávez & Ledeboer, 2007]. However, short chain oligosaccharides with low $T_g$ entail technological problems because they lead to the obtaining of sticky products that agglomerate and adhere to the internal wall of the drying chamber, resulting in low product yields and also decreasing bacterial viability [Sosa et al., 2016]. For this reason, higher molecular weight oligosaccharides and polysaccharides with higher $T_g$, such as maltodextrins, starch or inulins, are generally used to overcome such problems [Bhandari, Datta, & Howes, 1997; Fazaeli et al., 2012; Rajam & Anandharamakrishnan, 2015].

Amorphous inulin has been widely used to stabilize lactic acid bacteria during dehydration processes [Fritzen-Freire et al., 2013; Avila-Reyes, Garcia-Suarez, Jiménez, San Martín-Gonzalez, & Bello-Perez, 2014; Okuro, Thomazini, Balieiro, Liberal, & Fávaro-Trindade, 2013; Nunes et al., 2018; Corcoran, Ross, Fitzgerald, & Stanton, 2004], but its relatively low solubility limits the use of the obtained products in food formulation. Crystalline inulin gives more flowable dried products with a greater water dispersibility. However, to the best of our knowledge no attempts to investigate the role of highly crystalline inulin on bacterial stabilization have been carried out hereto. Therefore, the goal of this work was to elucidate the protective capacity of highly crystalline inulins during pilot scale spray-drying of *Lactobacillus plantarum* CIDCA 83114, and subsequent storage for 180 days at 20 °C. The strain was selected because of its inhibition properties on the growth and/or the activity of *E. coli* O157:H7, *Shigella* and *Salmonella* [Hugo, Kakisu, De Antoni, & Pérez, 2008; Golowczyc, Gerez, et al., 2011; Kakisu, Abraham, Tironi Farinati, Ibarra, & De Antoni, 2013; Kakisu, Bolla, Abraham, de Urraza, & De Antoni, 2013]. The stabilizing capacity of crystalline inulin powders was investigated on the bases of their physical properties (*i.e.*, melting temperatures, water sorption isotherms, water activity, and infrared light absorption). Scanning electronic and confocal microsopies provided a full landscape about the interactions between microorganisms and crystals, and also on the bacterial location within the amorphous matrices. The technological properties of the dehydrated microorganisms (culturability and acidification capacity) during storage at different water activities were also evaluated. In all cases, amorphous inulins were used as controls.

## 2. Materials and methods

### 2.1. Preparation of bacterial samples

*Lactobacillus plantarum* CIDCA 83114 was isolated from a fermented milk [Garrote, Abraham, & De Antoni, 2001]. The strain was maintained frozen at −80 °C in 120 g/L non-fat milk solids. Cultures were grown in 1 L of de Man, Rogosa, Sharpe (MRS) broth [de Man, Rogosa, & Sharpe, 1960] at 30 °C overnight in aerobic conditions, to obtain approximately $10^{10}$–$10^{11}$ CFU/mL (stationary phase). Then, they were harvested by centrifugation at 10000 ×*g* for 10 min at 4 °C, and the pellets were washed twice with 0.85% w/v NaCl and used for subsequent assays.

### 2.2. Obtaining amorphous and crystalline inulins

HP inulin, containing oligosaccharides with average DP (DPn) 23, was used (Raftilose HP, Orafti Beneo, Germany) [Schaller-Povolny, Smith, & Labuza, 2000]. The experimental protocol for obtaining amorphous and crystalline samples is shown in Scheme 1.

#### 2.2.1. Amorphous inulin samples

20% w/v suspensions of HP inulin were heated at 95 °C under shaking (100 rpm for 15 min) to eliminate the initial crystalline structures and allow a complete dissolution. Samples were then cooled down up to 30 °C without stirring, and used for subsequent assays.

#### 2.2.2. Crystalline inulin samples

In parallel assays, 20% w/v inulin solutions (at 95 °C) were stored at 4 °C for 72 h under stirring (100 rpm). Crystallization was monitored by registering the absorbance at 700 nm at regular intervals, in a UV–vis spectrophotometer (Shimadzu, Kyoto, Japan). The obtained crystals were centrifuged at 10000 ×*g* for 30 min, and kept for further analyses.

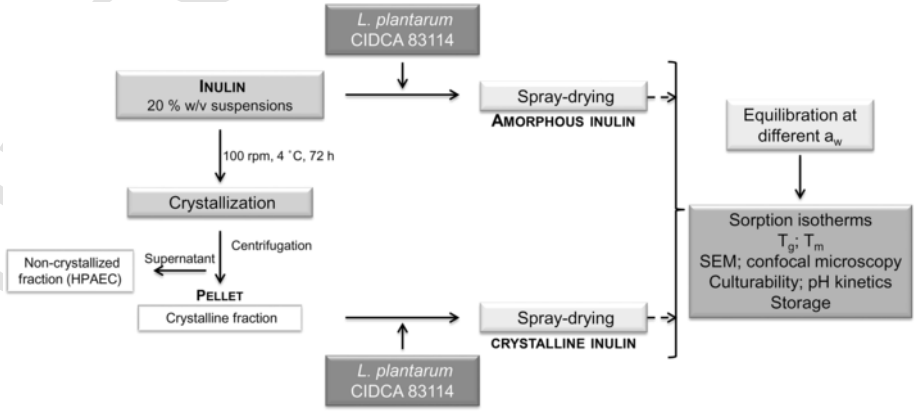


**Scheme 1.** Experimental protocol for obtaining amorphous and crystalline HP inulins containing *L. plantarum* CIDCA 83114.

The supernatants were referred as non-crystallized fraction. The composition of such fraction was determined by high performance anion exchange chromatography (HPAEC) according to Romano, Araujo-Andrade, Lecot, Mobili, and Gomez-Zavaglia (2018). External standards of fructose, glucose, sucrose, 1-kestose (DP3), nystose (DP4) and 1 F-fructofuranosylnystose (DP5) were used to determine their retention times and check the linear range of the measurements.

### 2.3. Spray drying

The bacterial pellets obtained in section 2.1 were incorporated into 1 L of 20% w/v amorphous or crystalline inulin samples (sections 2.2.1 and 2.2.2, respectively), achieving a bacterial concentration of $10^{10}$–$10^{11}$ CFU/mL. Samples were spray-dried at a pilot scale on an Armfield FT80 spray-dryer (DY, United Kingdom) at a constant air inlet temperature of 160 °C and an outlet temperature of 65 ± 5 °C.

### 2.4. Water activity ($a_w$) and humidity of samples

#### 2.4.1. $a_w$ measurements

The $a_w$ of the amorphous and crystalline inulins containing microorganisms obtained in section 2.3 was determined by using an Aqualab water activity instrument (Aqualab, Model Series 3TE, USA). The equipment was calibrated using standard salt solutions provided by the manufacturer

#### 2.4.2. Water sorption isotherms

2 g of the dehydrated samples of amorphous and crystalline inulins containing microorganisms obtained in section 2.3 were equilibrated at 20 °C in atmospheres of the following saturated salts: LiCl, $CH_3CO_2K$, $MgCl_2$, $K_2CO_3$, $Mg(NO_3)_2$, $NaNO_2$, NaCl, KCl and $K_2SO_4$, giving $a_w$ of 0.11, 0.22, 0.33, 0.40, 0.54, 0.64, 0.75, 0.84 and 0.97, respectively (Scheme 1). Moisture contents were determined by measuring their weight loss, upon drying at 105 °C until constant weight [AOAC, 1980]. Moisture results were expressed in grams of water per gram of dried matter (d.m.).

A Guggenheim-Anderson-de Boer (GAB) model was used to fit sorption isotherm data. GAB isotherm model can be expressed as follows:

$$M_w = \frac{M_o C K a_w (1 - Kaw + CKaw)}{(1 - Kaw)} \quad (1)$$

where $M_w$ is the equilibrium moisture content (g water/g dry matter) at a given $a_w$, $M_0$ is the monolayer value (g water/g dry matter) and $C$ and $K$ are the Guggenheim constant and the correction factor for the multilayer with respect to the bulk liquid, respectively [Perez-Alonso, Beristain, Lobato-Calleros, Rodriguez-Huezo, & Vernon-Carter, 2006].

### 2.5. Glass transition and melting temperatures ($T_g$, $T_m$)

The $T_g$ and $T_m$ of amorphous and highly crystalline samples containing microorganisms were determined by differential scanning calorimetry (DSC) using a Q100 calorimeter (TA Instruments, New Castle, DE, USA), calibrated with indium, lead and zinc. Hermetically sealed 40 μL medium pressure pans were used (an empty pan served as reference). The heating rate was 10 °C/min. Enthalpy values were reported for melting processes (Tm), and the middle temperatures, for vitrification ones ($T_g$). An average value of at least two replicates was informed.

### 2.6. Fourier transform infrared spectroscopy (FTIR)

FTIR spectra were registered at 20 °C on the amorphous and highly crystalline inulins containing microorganisms, and equilibrated at water activities within 0.11–0.97 (section 2.4). Approximately 5 mg of each sample were placed on the sample holder of an Attenuated Total Reflection FTIR (ATR-FTIR) Thermo Nicolet iS10 spectrometer (Thermo Scientific, MA, USA). Spectra were registered in the 4000–500 $cm^{-1}$ range by co-adding 100 scans with 4 $cm^{-1}$ spectral resolution, using OMNIC software (version 8.3, Thermo Scientific, MA, USA). At least 7 spectra were recorded for each sample.

### 2.7. Microscopic observations

#### 2.7.1. Scanning electronic microscopy (SEM)

All powder samples obtained in section 2.3 were examined with a FEI model Quanta 200 electron microscope (The Netherlands). Samples were mounted onto bronze stubs by using a double-sided tape and examined without any metal or carbon coating at low pressure and an acceleration voltage of 20.0 kV.

#### 2.7.2. Confocal laser scanning microscopy analysis

Microorganisms spray-dried in the presence of amorphous or highly crystalline inulin matrices were observed using a confocal laser-scanning microscope (Leica TCS SP5 Leica Microsystems, Wetzlar, Germany). Bacteria dehydrated in the presence of crystalline or amorphous inulin were suspended in distilled deionized water to attain a concentration of *ca.* $10^7$ cells/mL. Then, samples were fixed by adding 25% v/v methanol for 5 min at 20 °C to allow cell membrane permeabilization, and stained with To-Pro-3 iodide (DNA staining dye, final concentration: 1 mM) for 5 min at 37 °C. An aliquot of the suspension was dispersed on a glass slide and dried under a flow of sterile air. The excitation wavelength was 633 nm. Fresh cultures of *L. plantarum* CIDCA 83114 were used as controls.

### 2.8. Culturability of bacteria

Culturability of dehydrated samples (section 2.3), equilibrated at $a_w$ within 0.10 and 0.97 (section 2.4) was determined immediately after spray-drying, and during storage at 20 °C for 180 days. For each determination, samples were re-hydrated in 1 mL 0.85% w/v NaCl. Bacterial suspensions were serially diluted, plated on MRS agar, and incubated at 37 °C for 48 h in aerobic conditions.

### 2.9. Determination of the lag time

Spray-dried microorganisms were rehydrated in 1 mL of 0.85% w/v NaCl, immediately after dehydration and after 180 days of storage. The rehydrated microorganisms were inoculated in MRS broth (2% v/v inoculum) and incubated at 37 °C. Acidification kinetics were followed by determining the pH during 24 h.

### 2.10. Reproducibility of results

All experiments were performed on duplicate samples using three independent preparations. The relative differences were reproducible irrespective of the preparation employed. Analysis of variance (ANOVA) was carried out using the statistical program Infostat v2009 software (Córdoba, Argentina). Differences were tested with paired sample *t*-tests, and if $p < 0.05$ the difference was considered statistically significant.

## 3. Results and discussion

### 3.1. Characterization of amorphous and crystalline inulin matrices

Fig. 1 shows the crystallization kinetics of HP inulin, which adjusted to Eq. 2.

$$A = \frac{A1 - A2}{1 + \left(\frac{t}{c}\right)^{p}} + A2 \quad (2)$$

where $A$ is the absorbance at 700 nm at the time $t$; $t$, the time in hours; $A_1$, the initial absorbance at 700 nm ($t = 0$); $A_2$, the maximum absorbance achieved; $c$, the time corresponding to the inflection point, and $p$, an exponential fitting factor. The *lag* time of crystallization was calculated as the intersection of the tangent line at $t = c$ and $A_1$. The crystallization rate ($m$) during the exponential phase was calculated as the slope of the tangent line. After adjusting experimental data with Eq. 2, the following parameters were obtained: *lag* time (1.67 h), m (54.3 A.U./hour). $R^2$ was 0.99.

HP inulin solution, with DPn = 23, started crystallization rapidly, as evidenced by the short *lag* time (1.67 h) and the high crystallization rate ($m = 54.3$ A.U./hour), in agreement with Cooper, Barclay, Ginic-Markovic, Gerson, and Petrovsky (2014). In fact, these authors reported that clear inulin solutions (DPn~30) show a visible nucleation after 60 min, when dissolved at 85 °C and stirred at 5 °C. In turn, the non-crystallized fraction (section 2.2.2, Scheme 1) had high concentration of low DP oligosaccharides (Table S1), indicating that crystallization of inulin involved the interaction (nucleation) of high DP saccharides. Hence, the high DPn of HP inulin results in a fast nucleation and crystallization.

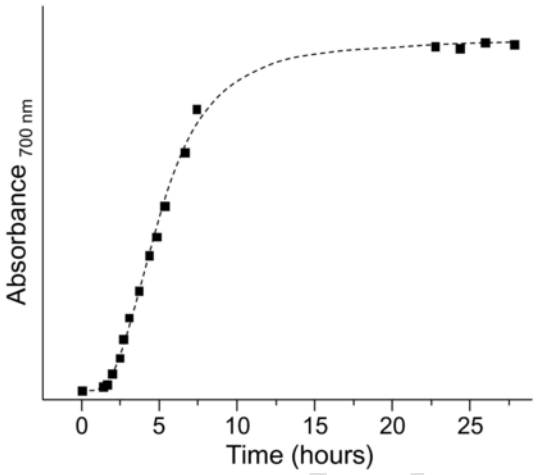


**Fig. 1.** Crystallization kinetics of 20% w/v solutions of HP inulin at 4 °C under stirring, as determined by registering their absorbance at 700 nm along time. Kinetic parameters: *lag* time (1.67 h), m (54.3 A.U./hour). $R^2 = 0.99$.

Table 1 shows the $T_g$ and $T_m$ of amorphous and crystalline HP inulins containing microorganisms. As expected, the $T_g$ of the amorphous states decreased as soon as the $a_w$ increased. Below $a_w$ 0.54, $T_g$ were high enough to ensure that when stored at 20 °C, samples remain in an amorphous state ($T\text{-}T_g < 0$). Regarding $T_m$, both amorphous and crystalline samples showed greater values as soon as $a_w$ increased, indicating that the higher the $a_w$, the greater the crystallinity of the samples. It is also important to underline that at $a_w < 0.54$, the $T_m$ of crystalline samples was significantly higher than that of amorphous ones, with no significant differences above that $a_w$ value ($p > 0.05$) (Table 1). Considering that as soon as $T\text{-}T_g$ decreases, amorphous inulins are more susceptible to caking and further crystallization [Aguilera, del Valle, & Karel, 1995; Roos, 2003], the greater crystalline character of such samples at $a_w > 0.54$ explains the similar $T_m$ values for amorphous and crystalline states (Table 1).

Fig. 2 depicts the FTIR spectra of the amorphous and crystalline inulins containing microorganisms, in the 1200–900 $cm^{-1}$ region (fingerprint region of sugars), at $a_w$ ranging from 0.11 to 0.97 and $T = 20$ °C. Broad bands characterized the spectra of amorphous inulins ($a_w < 0.54$) (Fig. 2A). The typical disorder of such states, creating an environment in which molecules can freely rotate, explains the broad character of the observed bands [Gomez-Zavaglia & Fausto, 2003]. When $T > T_g$, that is, at $a_w \geq 0.64$, the presence of water molecules and the high molecular mobility of oligosaccharides promoted a partial crystallization, which results in narrower bands, typical from the three-dimensional crystalline arrangements [Gomez-Zavaglia & Fausto, 2003], and is also consistent with the higher $T_m$ values, shown in Table 1. Bands occurring in the fingerprint region of sugars, that is, the region in which each individual sugar can be univocally identified, are essentially ascribed to the δCOH, the C—O—C glycosidic linkage, and the νC—C vibrational modes [Santos, Araujo-Andrade, Tymczyszyn, & Gómez-Zavaglia, 2014]. The band at 935 $cm^{-1}$ has been reported as typical from inulin, and ascribed to the β2→1 glycosidic bond [Barclay et al., 2016]. The increase in the intensity of such band, and that of the bands at 1037 and 995 $cm^{-1}$, is considered as indicative of molecular organization [Barclay et al., 2016], typical from the crystalline state. In addition, the band arising from the δCOH vibrational mode (1037 $cm^{-1}$), shifted to higher wavenumbers as $a_w$ increased (Fig. 2A, B), indicating the presence of stronger hydrogen-bonds (those established between sugars and water in the crystalline state) [Santos et al., 2014]. The greater changes in the spectra of amorphous matrices (Fig. 2A) can be ascribed to the presence of increasing amounts of water, which leads samples to crystallize. Crystallization of amorphous matrices is a well-known undesirable effect that strongly conditions their stability during dehydration and storage. Izutsu and Kojima (2002) reported that crystallization of mannitol during freeze-drying leads to

**Table 1**
Thermal properties of HP inulin in the amorphous and crystalline states, previously stabilized at 4 °C for 30 days at water activities ranging from 0.11 to 0.97.

| | Glass transition temperature ($T_g$) (°C) | | Enthalpy of fusion ($T_m$) (J/g) | |
|---|---|---|---|---|
| $a_w$ | Amorphous | Crystalline | Amorphous | Crystalline |
| 0.11 | 91.0 ± 1.9 | – | 28.4 ± 4.3 | 130.6 ± 6.7 |
| 0.22 | 71.1 ± 1.3 | – | 53.1 ± 20.6 | 144.2 ± 8.9 |
| 0.33 | 53.6 ± 10.2 | – | 121.0 ± 33.3 | 171.2 ± 23.1 |
| 0.40 | 50.7 ± 5.3 | – | 166.2 ± 28.6 | 176.3 ± 14.5 |
| 0.54 | 34.9 ± 0.8 | – | 195.9 ± 1.7 | 206.4 ± 27.7 |
| 0.64 | 15.4 ± 0.5 | – | 232.9 ± 43.6 | 238.3 ± 21.7 |
| 0.75 | 7.6 ± 0.3 | – | 303.4 ± 11.2 | 279.7 ± 5.1 |
| 0.84 | −23.4 ± 3.1 | – | 295.7 ± 36.2 | 280.8 ± 34.1 |
| 0.97 | −32.0 ± 2.1 | – | 410.3 ± 28.3 | 347.6 ± 9.4 |

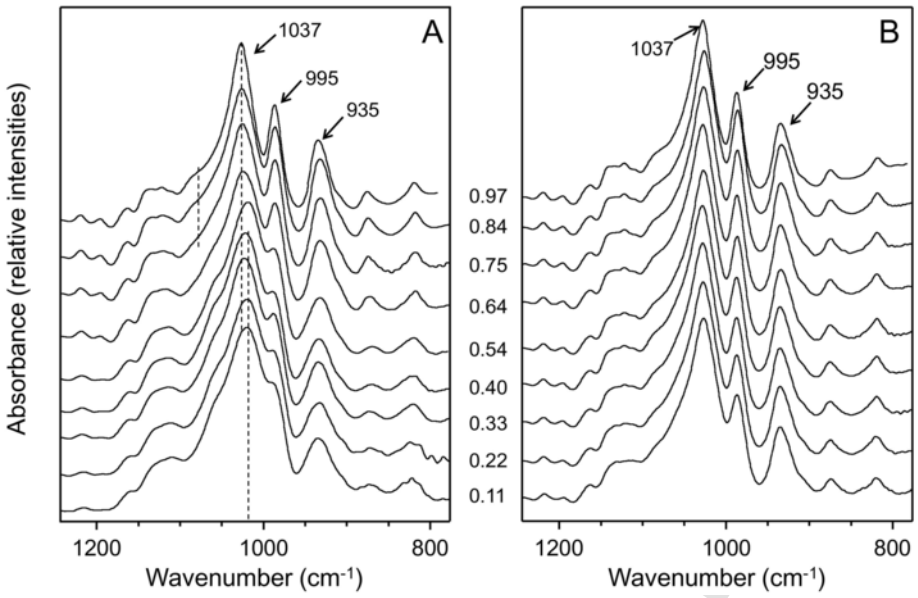


**Fig. 2.** FTIR spectra of HP inulin containing *L. plantarum* CIDCA 83114 in the 1200–900 $cm^{-1}$ region, immediately after spray-drying and equilibration at different $a_w$ (from 0.11 to 0.97) at 20 °C.A. amorphous inulinB. crystalline inulin

protein destabilization because it precludes the interaction sugar-protein. Passot, Cenard, Douania, Tréléa, and Fonseca (2012) informed that the crystallization of disaccharides induces an increase in $a_w$, due to the release of water from the amorphous sugar matrix, thus accelerating deteriorative changes, such as non-enzymatic browning [Passot et al., 2012].

Fig. 3 shows the sorption isotherms ($T = 20$ °C) of amorphous and crystalline inulin containing microorganisms. The GAB model (Eq. 1) was used to adjust the experimental data. Both isotherms presented the typical sigmoid shape type II isotherm [Al-Muhtaseb, McMinn, & Magee, 2002]. This behavior indicates that as moisture content increased, free water, represented by $a_w$, increased accordingly. The parameters of the GAB model, $M_0$, C and K are shown in Table 2. $M_0$ showed similar values for amorphous and crystalline inulins, indicating that both types of samples had similar water binding capacities at low $a_w$ [Zimeri & Kokini, 2002]. *K* value for amorphous inulin was greater than for crystalline one (Table 1). According to Schaller-Povolny et al. (2000), as the effective molecular weight of the inulin decreased, the *K* values of the GAB model increased, indicating a shift from the Type II to the Type III isotherm curve. This may be due to the fact that amorphous inulin is enriched by low DP molecules (Table S1), which have more hydroxyl groups available to bind water in comparison with crystalline inulin, in which the low DP fraction has been removed. As a result, the sigmoidal shape of the Type II isotherm curve seems like a flat shape Type III isotherm curve, typical from amorphous sugars [Schaller-Povolny et al., 2000; Al-Muhtaseb et al., 2002; Ronkart et al., 2006]. A greater increase in the moisture content of amorphous inulin powder was observed at $a_w \geq 0.64$, where $T > T_g$ (Table 1), leading to caking and crystallization (Figs. 2, 3; Table 1).

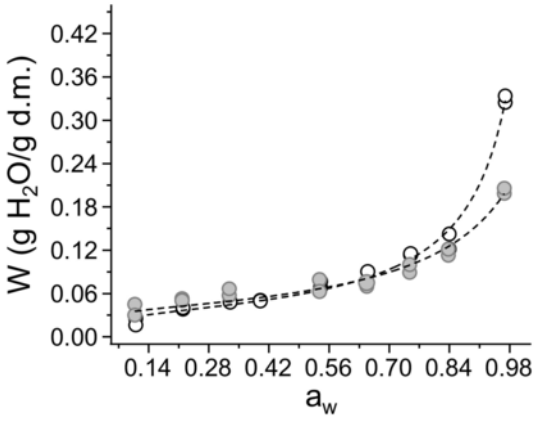


**Fig. 3.** Adsorption isotherms of water vapor on HP inulin containing *L. plantarum* CIDCA 83114. Samples were previously equilibrated at $0.11 < a_w < 0.97$ at 20 °C, for 30 days. White circles (amorphous inulin); gray circles (crystalline inulin).

**Table 2**
Parameters of the GAB equation (Eq. 1).

| GAB parameters | Amorphous inulin | Crystalline inulin |
|---|---|---|
| $M_0$ | 0.034 ± 0.001 | 0.037 ± 0.002 |
| C | 20.9 ± 1.8 | 65.5 ± 5.2 |
| K | 0.924 ± 0.004 | 0.836 ± 0.013 |

### 3.2. *Effect of amorphous and crystalline inulin matrices during spray-drying of L. plantarum CIDCA 83114*

Fig. 4 shows the microscopic images of amorphous and crystalline inulin matrices containing microorganisms.

Crystalline structures were observed in both inulin forms. The presence of small crystals (diameter below 2.17 μm) in the amorphous form can be explained considering the high DP of the HP inulin and the spray-drying conditions. In fact, the high air inlet temperature (160 °C) and quick cooling down to the outlet temperature (65 °C) favored the crystal formation. No aggregates were observed in the amorphous state (Fig. 4A). In turn, crystalline inulin showed crystals of different diameters, and aggregates (Fig. 4B). Small crystals had diameters within 0.87 and 2.17 μm, and large crystals had diameters within 3.33 and 7.49 μm. In addition, aggregates composed of more than one type of crystal were also observed (Fig. 4B).

The presence of the microorganisms in the inulin matrices was determined using confocal laser-scanning microscopy (Fig. 5). Amorphous inulin showed microorganisms and no crystals, which can be explained considering that just a few small crystals were present in such

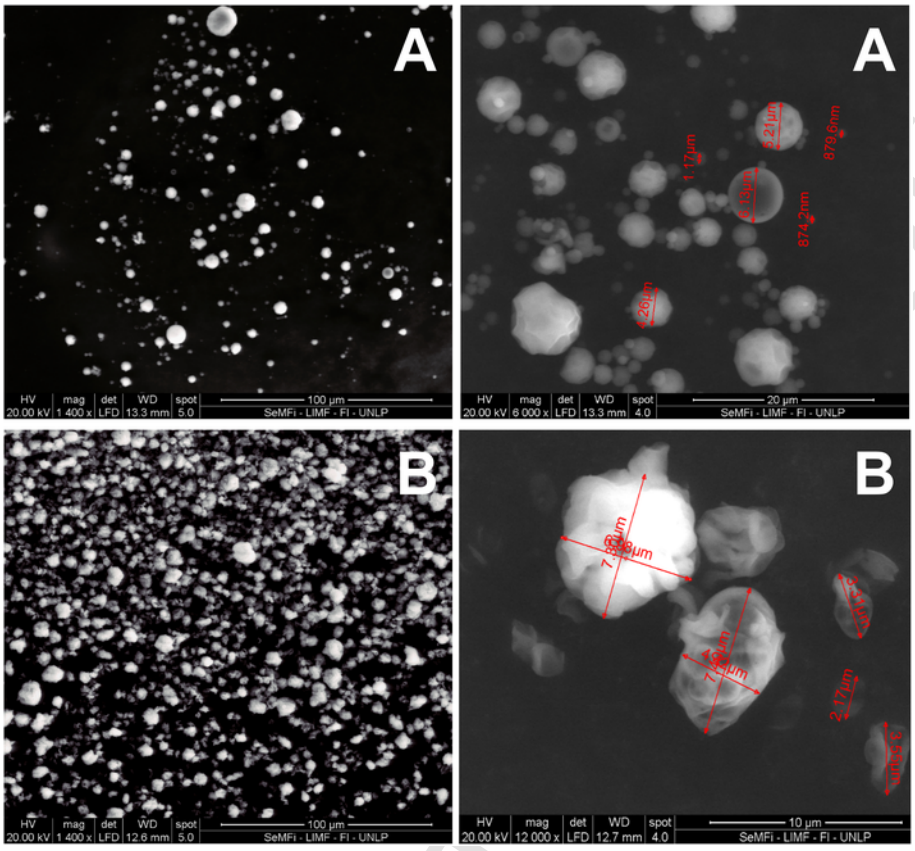


**Fig. 4.** SEM micrographs of dehydrated inulin containing *L. plantarum* CIDCA 83114. Images on the same row correspond to different magnifications of the same sample.A. amorphous inulinB. crystalline inulinThe diameters of some of the crystals were denoted in red. (For interpretation of the references to color in this figure legend, the reader is referred to the web version of this article.)

matrices (Fig. 5A). On the contrary, samples with crystalline matrix contained both microorganisms and high amounts of crystals (Fig. 5B).

Fig. S1 shows the culturability of microorganisms spray-dried in amorphous or crystalline inulin matrices. Fresh cultures (bacteria before spray-drying) had 11.11 ± 1.96 log CFU/g. The culturability slightly decrease after the process (9.74 ± 0.20 log CFU/g for crystalline inulin and 9.93 ± 1.61 log CFU/g for the amorphous matrices), with no significance differences arising from the physical state of the matrices. It is worth to mention that amorphous inulin matrices showed an accumulation of insoluble inulin at the bottom of the tube, after suspending the spray-dried powders in water. This was not observed for crystalline samples (Fig. S2).

Fig. 6 depicts the culturability of *L. plantarum* CIDCA 83114 in amorphous and crystalline inulin matrices during storage at 20 °C and different $a_w$. At $a_w < 0.33$, no significant decrease in culturability was observed after 180 days of storage, both in the amorphous and in the crystalline state. In both amorphous and crystalline matrices, two different groups were observed. One of them, composed of samples stored at $a_w < 0.40$, and the second one, much less stable, integrated by microorganisms stored above that $a_w$ value (Figs. 6A, B). It is important to point out that in this latter group, bacteria spray-dried in crystalline matrices were still culturable after 30 days of storage at $a_w$ 0.75 (5.39 ± 0.55 log CFU/g). Fig. S3 shows the behavior of inactivation constants ($k$) at different $a_w$ values. At $a_w < 0.40$, no significant differences between $k$ values of amorphous and crystalline samples were observed. At higher $a_w$ values, the inactivation constants of amorphous samples were significantly greater than those of the crystalline ones (Table S2).

MRS culture acidification kinetics of amorphous and crystalline samples immediately after spray-drying and after 180 days of storage at 20 °C are shown in Fig. S4. Kinetics were adjusted according to Eq. 3:

$$pH(t) = \frac{pH_o - pH_f}{1 + \left(\frac{t}{c}\right)^p} + pH_f \quad (3)$$

where $t$ is the time in hours, $pH_0$, the pH at $t = 0$, $pH_f$, the pH once attained the stationary phase, $c$, the time corresponding to the inflection point, and $p$, an exponential fitting factor (Table S3). The kinetics were consistent with the stability of samples during storage (Fig. 6). The higher the $a_w$, the lower the medium acidification rate, and the longer the *lag* times. This behavior can be explained considering the greater destabilization of amorphous samples when T-$T_g$ is close to zero [Santos et al., 2014]. $T_g$ itself is important only as a macroscopic parameter, and for an adequate preservation of food and food related products, low molecular mobility is also required. In practice, the low molecular mobility is attained at low water contents and low storage temperatures [Tromp, Parker, & Ring, 1997; Schoonman, Ubbink, Bisperink, Le Meste, & Karel, 2002; Tymczyszyn et al., 2012]. Therefore, T-$T_g$ is very important because it is directly related to the shelf-life of starters and food products [Tymczyszyn et al., 2012]. This indicates that the best storage condition will be that at which the temperature of storage is as far as possible below $T_g$. For this reason, the evaluation of long term culturability requires the consideration of both storage temperature (T) and $T_g$ for amorphous matrices. This appears as a limitation in conditions at which amorphous samples started to crystallize (Figs. 2,3,6A, Fig. S3 and Table 1). In fact, crystallization of amorphous samples has been reported to destabilize microorganisms during

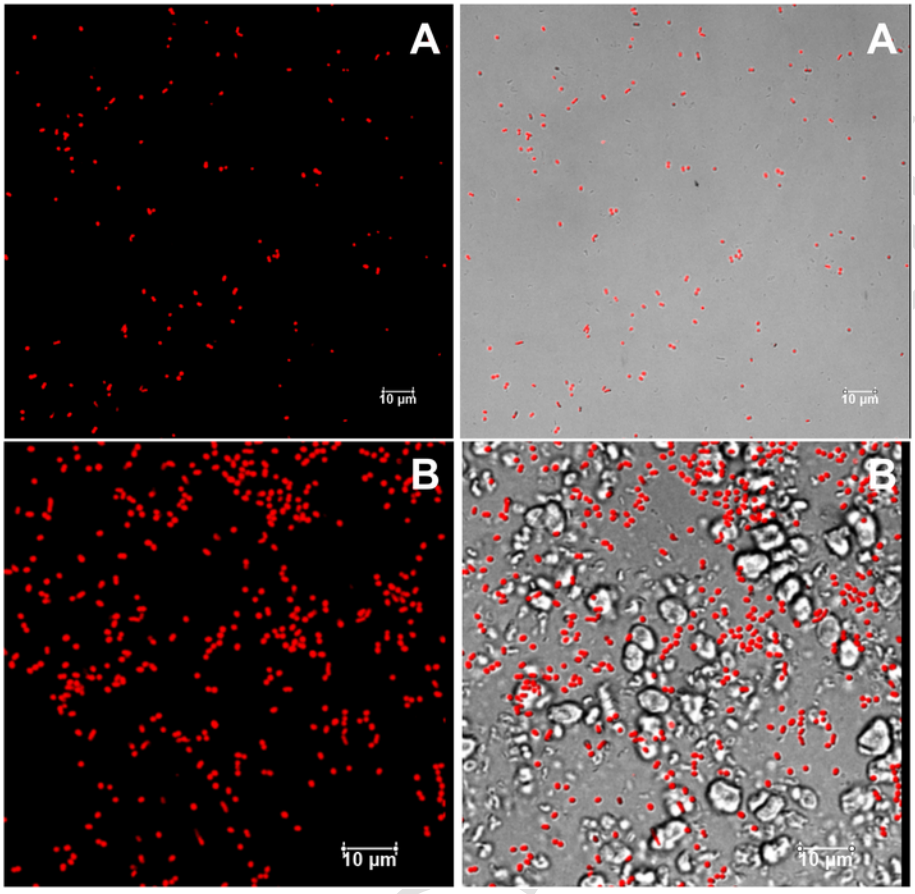


**Fig. 5.** Confocal microscopy images of *L. plantarum* CIDCA 83114 in a matrix of inulin. Images on the left correspond to the fluorescence from the To-Pro-3 probe inside the microorganisms at 633 nm. Images on the right are the result of superimposing fluorescence images to light field images.A. amorphous inulinB. crystalline inulin

storage [Passot et al., 2012]. In such conditions, the presence of water induces deteriorative biochemical reactions, with a harmful effect on microorganisms [Izutsu & Kojima, 2002]. This undesirable effect was not observed during storage of *L. plantarum* CIDCA 83114 in crystalline inulin structures (Fig. 6B and Fig. S3). Contrarily to amorphous structures that crystalized during storage, crystals obtained under controlled conditions of temperature, time and shaking (see section 2.2.2), result in highly organized structures. As the molecular mobility is low in such structures, deteriorative reactions become slower and thus, microorganisms were better stabilized.

## 4. Conclusions

The effect of amorphous and crystalline inulins as protective matrices of *L. plantarum* CIDCA 83114 was assessed. The physico-chemical properties of both inulin states explained their behavior during bacterial pilot spray-drying and storage. Bacterial stabilization was directly related to inulin stabilization.

As shown in this work, crystalline inulin was more stable than amorphous one, especially at the highest $a_w$, when T was close to $T_g$ in amorphous samples. This resulted in a better matrix to protect microorganisms during pilot spray-drying and storage. Moreover, the dispersibility of crystalline inulin after suspending the spray-dried samples (Fig. S2) outcomes an additional clear advantage over the amorphous one. This was the first time that such protective effect was reported.

Considering the physico-chemical advantageous properties of crystalline inulin, and the probiotic properties of *L. plantarum* CIDCA 83114, the integrated approach developed in this work (both from a fundamental and from an applied viewpoint), supports their incorporation as functional ingredients in the formulation of novel functional food products.

Supplementary data to this article can be found online at https://doi.org/10.1016/j.foodres.2018.07.007.

## Uncited reference

Rajam et al., 2015

## Acknowledgments

This work was supported by the Argentinean Agency for the Scientific and Technological Promotion (ANPCyT) (Projects PICT/2014/0912), and the bilateral project Chile-Argentina (Conicyt-Mincyt Ch-13-02). Eng. Javier Lecot, Claudio Reyes and Lib. Diana Velasco (CIDCA, Argentina), and Eng. Victor Muñoz and Alonso Godoy (CREAS, Chile) are acknowledged for technical assistance. P.M. and A.G.-Z. are members of the research career CONICET. N.R. is postdoctoral fellow from CONICET.

## Competing interests

The authors declare that they have no competing interests.

## Author's contributions

N.R. conceived the work. N.R and P.M. did the experimental work. A.G.-Z and M.E.Z.-H. coordinated the work (analysis of results, discus-

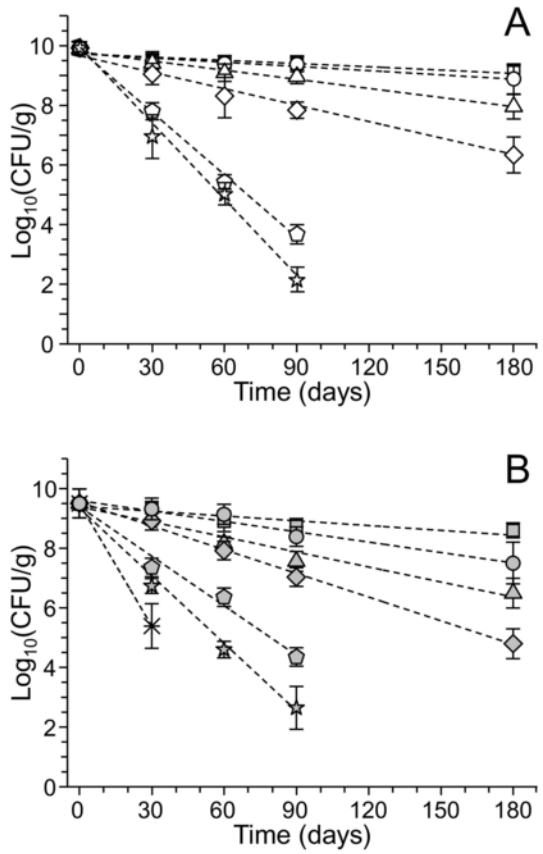


**Fig. 6.** MRS agar culturability, expressed as log CFU/g of *L. plantarum* CIDCA 83114 in a matrix of inulin, immediately after spray-drying (day 0), and during storage at 20 °C. During storage, samples were equilibrated at different water activities: 0.11 (squares), 0.22 (circles), 0.33 (triangles), 0.40 (diamonds), 0.54 (pentagons), 0.65 (stars), 0.75 (asterisks).A. amorphous inulinB. crystalline inulin

sion and writing of the manuscript). All authors have approved the final version of the manuscript.

## References

Aguilera, J., del Valle, J., Karel, M., 1995. Caking phenomena in amorphous food powders. Trends in Food Science & Technology 6, 149–155.

Al-Muhtaseb, A.H., McMinn, W.A.M., Magee, T.R.A., 2002. Moisture sorption isotherm characteristics of food products: a review. Food and bioproducts processing. Vol. 80, 118–128.

AOAC Official methods of analysis, 1980. Association of official analytical chemists, 13th ed, (Washington, DC).

Avila-Reyes, S.V., Garcia-Suarez, F.J., Jiménez, M.T., San Martín-Gonzalez, M.F., Bello-Perez, L.A., 2014. Protection of L. rhamnosus by spray-drying using two prebiotics colloids to enhance the viability. Carbohydrate Polymers 102, 423–430.

Barclay, G., Rajapaksha, H., Thilagam, A., Qian, G., Ginic-Markovic, M., Cooper, P.D., … Petrovsky, N., 2016. Physical characterization and in silico modeling of inulin polymerconformation during vaccine adjuvant particle formation. Carbohydrate Polymers 143, 108–115.

Bhandari, B.R., Datta, N., Howes, T., 1997. Problems associated with spray-drying of sugar-rich foods. Drying Technology 15, 671–684.

Chávez, B.E., Ledeboer, A.M., 2007. Drying of probiotics: optimization of formulation and process to enhance storage survival. Drying Technology 25, 1193–1201.

Cooper, P.D., Barclay, T.G., Ginic-Markovic, M., Gerson, A.R., Petrovsky, N., 2014. Inulin isoforms differ by repeated additions of one crystal unit cell. Carbohydrate Polymers 103, 392–397.

Corcoran, B.M., Ross, R.P., Fitzgerald, G.F., Stanton, C., 2004. Comparative survival of probiotic lactobacilli spray-dried in the presence of prebiotic substances. Journal of Applied Microbiology 96, 1024–1039.

Crowe, J.H., Carpenter, J.F., Crowe, L.M., 1998. The role of vitrification in anhydrobiosis. Annual Reviews on Physiology 60, 73–103.

Fazaeli, M., Emam-Djomeh, Z., Ashtari, A.K., Omid, M., 2012. Effect of spray-drying conditions and feed composition on the physical properties of black mulberry juice powder. Food and bioproducts processing. Vol. 90, 667–675.

Franck, A., 2002. Technological functionality of inulin and oligofructose. British Journal of Nutrition 87, S287–S291.

Fritzen-Freire, C.B., Prudêncio, E.S., Pinto, S.S., Muñoz, I.B., Müller, C.M., Vieira, C.R., Amboni, R.D., 2013. Effect of the application of Bifidobacterium BB-12 microencapsulated by spray-drying with prebiotics on the properties of ricotta cream. Food Research International 52, 50–55.

Garrote, G.L., Abraham, A.G., De Antoni, G.L., 2001. Chemical and microbiological characterisation of kefir grains. Journal of Dairy Research 68, 639–652.

Golowczyc, M., Silva, J., Teixeira, P., De Antoni, G., Abraham, A., 2011. Cellular injuries of spray-dried Lactobacillus spp. isolated from kefir and their impact on probiotic properties. International Journal of Food Microbiology 144, 556–560.

Golowczyc, M.A., Gerez, C.L., Silva, J., Abraham, A.G., De Antoni, G.L., Teixeira, P., 2011. Survival of spray-dried Lactobacillus kefir is affected by different protectants and storage conditions. Biotechnology Letters 33, 681–686.

Gomez-Zavaglia, A., Fausto, R., 2003. Low temperature solid-state FTIR study of glycine, sarcosine and N,N-dimethylglycine: observation of neutral forms of simple α-aminoacids in the solid state. Physical Chemistry Chemical Physics 5, 3154–3161.

Hinrichs, W.L., Prinsen, M.G., Frijlink, H.W., 2001. Inulin glasses for the stabilization of therapeutic proteins. International Journal of Pharmaceutics 215, 163–174.

Hugo, A.A., Kakisu, E., De Antoni, G.L., Pérez, P.F., 2008. Lactobacilli antagonize biological effects of enterohaemorrhagic Escherichia coli in vitro. Letters in Applied Microbiology 46, 613–619.

Izutsu, K.I., Kojima, S., 2002. Excipient crystallinity and its protein-structure-stabilizing effect during freeze-drying. Journal of Pharmacy and Pharmacology 54, 1033–1039.

Kakisu, E., Abraham, A.G., Tironi Farinati, C., Ibarra, C., De Antoni, G.L., 2013. Lactobacillus plantarum isolated from kefir protects vero cells from cytotoxicity by type-II Shiga toxin from Escherichia coli O157:H7. Journal of Dairy Research 80, 64–71.

Kakisu, E., Bolla, P., Abraham, A.G., de Urraza, P., De Antoni, G.L., 2013. Lactobacillus plantarum isolated from kefir: Protection of cultured Hep-2 cells against Shigella invasion. International Dairy Journal 33, 22–26.

Kaur, N., Gupta, A., 2002. Applications of inulin and oligofructose in health and nutrition. Journal of Biosciences 27, 703–714.

Kelly, G., 2008. Inulin-type prebiotics. A review: part 1. Alternative Medicine Review 13, 315–329.

Kelly, G., 2009. Inulin-type prebiotics. A review: part 1. Alternative Medicine Review 14, 36–55.

Kolida, S., Gibson, G.R., 2007. Prebiotic capacity of inulin-type fructans. Journal of Nutrition 137, 2503S–2506S.

de Man, J.C., Rogosa, M., Sharpe, M.E., 1960. A medium for the cultivation of lactobacilli. Journal of Applied Bacteriology 23, 130–135.

Meng, X.C., Stanton, C., Fitzgerald, G.F., Daly, C., Ross, R.P., 2008. Anhydrobiotics: The challenges of drying probiotic cultures. Food Chemistry 106, 1406–1416.

Meyer, D., Bayarri, S., Tárrega, A., Costell, E., 2011. Inulin as texture modifier in dairy products. Food Hydrocolloids 25, 1881–1890.

Morgan, C.A., Herman, N., White, P.A., Vesey, G., 2006. Preservation of micro-organisms by drying: A review. Journal of Microbiolical Methods 66, 183–193.

Nunes, G.L., Etchepare, M.A., Cichoski, A.J., Zepka, L.Q., Lopes, E.J., Barin, J.S., … de Menezes, C.R., 2018. Inulin, hi-maize, and trehalose as thermal protectants for increasing viability of Lactobacillus acidophilus encapsulated by spray-drying. LWT-Food Science and Technology 89, 128–133.

Okuro, P.K., Thomazini, M., Balieiro, J.C., Liberal, R.D., Fávaro-Trindade, C.S., 2013. Co-encapsulation of Lactobacillus acidophilus with inulin or polydextrose in solid lipid microparticles provides protection and improves stability. Food Research International 53, 96–103.

Passot, S., Cenard, S., Douania, I., Tréléa, I.C., Fonseca, F., 2012. Critical water activity and amorphous state for optimal preservation of lyophilised lactic acid bacteria. Food Chemistry 132, 1699–1705.

Perez-Alonso, C., Beristain, C.I., Lobato-Calleros, C., Rodriguez-Huezo, M.E., Vernon-Carter, E.J., 2006. Thermodynamic analysis of the sorption isotherms of pure and blended carbohydrate polymers. Journal of Food Engineering 77, 753–760.

Quintana, G., Gerbino, E., Gomez-Zavaglia, A., 2017. Okara: A nutritionally valuable by-product able to stabilize Lactobacillus plantarum during freeze-drying, spray-drying, and storage. Frontiers in Microbiology 8, 641–650.

Rajam, R., Anandharamakrishnan, C., 2015. Microencapsulation of Lactobacillus plantarum (MTCC 5422) with fructooligosaccharide as wall material by spray-drying. LWT- Food Science and Technology 60, 773–780.

Rajam, R., Kumar, S.B., Prabhasankar, P., Anandharamakrishnan, C., 2015. Microencapsulation of Lactobacillus plantarum MTCC 5422 in fructooligosaccharide and whey protein wall systems and its impact on noodle quality. Journal of Food Science and Technology 52, 4029–4041.

Roberfroid, M.B., Delzenne, N.M., 1998. Dietary fructans. Annual Review of Nutrition 18, 117–143.

Romano, N., Araujo-Andrade, C., Lecot, J., Mobili, P., Gomez-Zavaglia, A., 2018. Infrared spectroscopy as an alternative methodology to evaluate the effect of structural features on the physical-chemical properties of inulins. Food Research International 109, 223–231.

Romano, N., Santos, M., Mobili, P., Vega, R., Gómez-Zavaglia, A., 2016. Effect of sucrose concentration on the composition of enzymatically synthesized short-chain fructo-oligosaccharides as determined by FTIR and multivariate analysis. Food Chemistry 202, 467–475.

Ronkart, S., Blecker, C., Fougnies, C., van Herck, J.C., Wouters, J., Paquot, M., 2006. Determination of physical changes of inulin related to sorption isotherms: An X-ray diffraction, modulated differential scanning calorimetry and environmental scanning electron microscopy study. Carbohydrate Polymers 63, 210–217.

Roos, Y., 2003. Thermal analysis, state transitions and food quality. Journal of Thermal Analysis and Calorimetry 71, 197–203.

Santivarangkna, C., Higl, B., Foerst, P., 2008. Protection mechanisms of sugars during different stages of preparation process of dried lactic acid starter cultures. Food Microbiology 25, 429–441.

Santos, M.I., Araujo-Andrade, C., Tymczyszyn, E.E., Gómez-Zavaglia, A., 2014. Determination of amorphous/rubbery states in freeze-dried prebiotic sugars using a com-

bined approach of near-infrared spectroscopy and multivariate analysis. Food Research International 64, 514–519.
Schaller-Povolny, L.A., Smith, D.E., Labuza, T.P., 2000. Effect of water content and molecular weight on the moisture isotherms and glass transition properties of inulin. International Journal of Food Properties 3, 173–192.
Schoonman, A., Ubbink, J., Bisperink, C., Le Meste, M., Karel, M., 2002. Solubility and diffusion of nitrogen in maltodextrin/protein tablets. Biotechnology Progress 18, 139–154.
Seifert, S., Watzl, B., 2007. Inulin and oligofructose: review of experimental data on immune modulation. Journal of Nutrition 137, 2563S–2567S.
Sosa, N., Gerbino, E., Golowczyc, M.A., Schebor, C., Gómez-Zavaglia, A., Tymczyszyn, E.E., 2016. Effect of galacto-oligosaccharides:maltodextrin matrices on the recovery of Lactobacillus plantarum after spray-drying. Frontiers in Microbiology 7, 584–592.
Tromp, R.H., Parker, R., Ring, S.G., 1997. Water diffusion in glasses of carbohydrates. Carbohydrate Research 303, 199–205.
Tymczyszyn, E.E., Sosa, N., Gerbino, E., Hugo, A., Gómez-Zavaglia, A., Schebor, C., 2012. Effect of physical properties on the stability of Lactobacillus bulgaricus in a freeze-dried galacto-oligosaccharides matrix. International Journal of Food Microbiology 155, 217–221.
Zimeri, J.E., Kokini, J.L., 2002. The effect of moisture content on the crystallinity and glass transition temperature of inulin. Carbohydrate Polymers 48, 299–304.

HP inulin solution, with DPn = 23, started crystallization rapidly, as evidenced by the short *lag* time (1.67 h) and the high crystallization rate ($m$ = 54.3 A.U./hour), in agreement with Cooper, Barclay, Ginic-Markovic, Gerson, and Petrovsky (2014). In fact, these authors reported that clear inulin solutions (DPn~30) show a visible nucleation after 60 min, when dissolved at 85 °C and stirred at 5 °C. In turn, the non-crystallized fraction (section 2.2.2, Scheme 1) had high concentration of low DP oligosaccharides (Table S1), indicating that crystallization of inulin involved the interaction (nucleation) of high DP saccharides. Hence, the high DPn of HP inulin results in a fast nucleation and crystallization.

Fig. 3 shows the sorption isotherms ($T$ = 20 °C) of amorphous and crystalline inulin containing microorganisms. The GAB model (Eq. 1) was used to adjust the experimental data. Both isotherms presented the typical sigmoid shape type II isotherm [Al-Muhtaseb, McMinn, & Magee, 2002]. This behavior indicates that as moisture content increased, free water, represented by $a_w$, increased accordingly. The parameters of the GAB model, $M_0$, C and K are shown in Table 2. $M_0$ showed similar values for amorphous and crystalline inulins, indicating that both types of samples had similar water binding capacities at low $a_w$ [Zimeri & Kokini, 2002]. $K$ value for amorphous inulin was greater than for crystalline one (Table 1). According to Schaller-Povolny et al. (2000), as the effective molecular weight of the inulin decreased, the $K$ values of the GAB model increased, indicating a shift from the Type II to the Type III isotherm curve. This may be due to the fact that amorphous inulin is enriched by low DP molecules (Table S1), which have more hydroxyl groups available to bind water in comparison with crystalline inulin, in which the low DP fraction has been removed. As a result, the sigmoidal shape of the Type II isotherm curve seems like a flat shape Type III isotherm curve, typical from amorphous sugars [Schaller-Povolny et al., 2000; Al-Muhtaseb et al., 2002; Ronkart et al., 2006]. A greater increase in the moisture content of amorphous inulin powder was observed at $a_w \geq 0.64$, where $T > T_g$ (Table 1), leading to caking and crystallization (Figs. 2, 3; Table 1).

Fig. S1 shows the culturability of microorganisms spray-dried in amorphous or crystalline inulin matrices. Fresh cultures (bacteria before spray-drying) had 11.11 ± 1.96 log CFU/g. The culturability slightly decrease after the process (9.74 ± 0.20 log CFU/g for crystalline inulin and 9.93 ± 1.61 log CFU/g for the amorphous matrices), with no significance differences arising from the physical state of the matrices. It is worth to mention that amorphous inulin matrices showed an accumulation of insoluble inulin at the bottom of the tube, after suspending the spray-dried powders in water. This was not observed for crystalline samples (Fig. S2).

Fig. 6 depicts the culturability of *L. plantarum* CIDCA 83114 in amorphous and crystalline inulin matrices during storage at 20 °C and different $a_w$. At $a_w < 0.33$, no significant decrease in culturability was observed after 180 days of storage, both in the amorphous and in the crystalline state. In both amorphous and crystalline matrices, two different groups were observed. One of them, composed of samples stored at $a_w < 0.40$, and the second one, much less stable, integrated by microorganisms stored above that $a_w$ value (Figs. 6A, B). It is important to point out that in this latter group, bacteria spray-dried in crystalline matrices were still culturable after 30 days of storage at $a_w$ 0.75 (5.39 ± 0.55 log CFU/g). Fig. S3 shows the behavior of inactivation constants ($k$) at different $a_w$ values. At $a_w < 0.40$, no significant differences between $k$ values of amorphous and crystalline samples were observed. At higher $a_w$ values, the inactivation constants of amorphous samples were significantly greater than those of the crystalline ones (Table S2).

MRS culture acidification kinetics of amorphous and crystalline samples immediately after spray-drying and after 180 days of storage at 20 °C are shown in Fig. S4. Kinetics were adjusted according to Eq. 3:

$$pH(t) = \frac{pH_o - pH_f}{1 + \left(\frac{t}{c}\right)^p} + pH_f \quad (3)$$

where $t$ is the time in hours, $pH_0$, the pH at $t = 0$, $pH_f$, the pH once attained the stationary phase, $c$, the time corresponding to the inflection point, and $p$, an exponential fitting factor (Table S3). The kinetics were consistent with the stability of samples during storage (Fig. 6). The higher the $a_w$, the lower the medium acidification rate, and the longer the *lag* times. This behavior can be explained considering the greater destabilization of amorphous samples when T-$T_g$ is close to zero [Santos et al., 2014]. $T_g$ itself is important only as a macroscopic parameter, and for an adequate preservation of food and food related products, low molecular mobility is also required. In practice, the low molecular mobility is attained at low water contents and low storage temperatures [Tromp, Parker, & Ring, 1997; Schoonman, Ubbink, Bisperink, Le Meste, & Karel, 2002; Tymczyszyn et al., 2012]. Therefore, T-$T_g$ is very important because it is directly related to the shelf-life of starters and food products [Tymczyszyn et al., 2012]. This indicates that the best storage condition will be that at which the temperature of storage is as far as possible below $T_g$. For this reason, the evaluation of long term culturability requires the consideration of both storage temperature (T) and $T_g$ for amorphous matrices. This appears as a limitation in conditions at which amorphous samples started to crystallize (Figs. 2,3,6A, Fig. S3 and Table 1). In fact, crystallization of amorphous samples has been reported to destabilize microorganisms during storage [Passot et al., 2012]. In such conditions, the presence of water induces deteriorative biochemical reactions, with a harmful effect on microorganisms [Izutsu & Kojima, 2002]. This undesirable effect was not observed during storage of *L. plantarum* CIDCA 83114 in crystalline inulin structures (Fig. 6B and Fig. S3). Contrarily to amorphous structures that crystalized during storage, crystals obtained under controlled

conditions of temperature, time and shaking (see section 2.2.2), result in highly organized structures. As the molecular mobility is low in such structures, deteriorative reactions become slower and thus, microorganisms were better stabilized.

As shown in this work, crystalline inulin was more stable than amorphous one, especially at the highest $a_w$, when T was close to $T_g$ in amorphous samples. This resulted in a better matrix to protect microorganisms during pilot spray-drying and storage. Moreover, the dispersibility of crystalline inulin after suspending the spray-dried samples (Fig. S2) outcomes an additional clear advantage over the amorphous one. This was the first time that such protective effect was reported.